RSC Advances

ROYAL SOCIETY OF CHEMISTRY

www.rsc.org/advances

Analysis of steady state and non-steady state corneal permeation of diclofenac

Rajaram Mohapatra[a], Subrata Mallick[a]*, Ashirbad Nanda[a], Rudra N Sahoo[a], Arunima Pramanik[a], Anindya Bose[a], Debajyoti Das[a], Lolly Pattnaik[b]

[a]School of Pharmaceutical Sciences, Siksha 'O' Anusandhan University, Kalinganagar, Bhubaneswar-751003, Orissa, India.

[b] Institute of Medical Sciences and Sum Hospital, Siksha 'O' Anusandhan University, Kalinganagar, Bhubaneswar-751003, Orissa, India.

---

*_Correspondence to_: SubrataMallick (Telephone: +91-674-2386209; fax: +91-674 2386271;

E-mail: subratamallick@soauniversity.ac.in; s_mallickin@yahoo.com; profsmallick@gmail.com

Abstract

The present study was undertaken for characterizing the steady state and non steady state corneal permeation kinetics of diclofenac potassium (DCP) using statistical moment theory. Hydrogel films containing DCP in hydroxypropyl methylcellulose (HPMC) matrix were prepared by casting method and the steady state and non-steady state corneal permeation parameters of diclofenac was evaluated using statistical moment analysis. Correlation coefficient (*r*), coefficient of non-determination and standard error of estimate (SEE) results indicated a good Level "A" correlation between in-vitro dissolution and ex-vivo steady state permeation of DCP from all the hydrogel formulations. SEM, XRD and DSC studies suggested the inhibition of the crystal growth and partial amorphization of diclofenac in the film. One way analysis of variance (ANOVA) followed by Dunnett's test revealed that all the hydrogel films containing plasticizer (L2, L3 and L4) have shown very high significant difference of extent of permeation in non-steady state (EPN), extent of permeation in lag time (EPL), extent of permeation in steady state (EPS) and total amount permeated in 360 min (TAP) from the control film containing no plasticizer (L1) related to highly improved permeation. Marked anti-inflammatory activity has been observed after application of the hydrogel film. Binding configuration of DCP-HPMC using docking calculation indicated drug-excipient interaction at molecular level. Steady state and non-steady state corneal permeation parameter has been evaluated successfully using statistical moment analysis and highly improved permeation has been observed when compared the parameters of the film with the control.

Keywords: Statistical moment analysis; Steady state; Non steady state; Triethanolamine; Hydrogel film.

1. Introduction

Ocular drug delivery is the most common treatment for diseases and disorders of the cornea such as allergies, conjunctivitis,corneal infections, dry eye, glaucoma etc**.** But the bioavailability of topically administered drugs is very poor due to low permeability of the multi-layered cornea[1,2], rapid nasolacrimal drainage, and absorption into the conjunctiva. Himmelstein et al. and Miller et al developed ocular physiological models[3,4]. Efficiency of new topical agents has been predicted widely using pharmacokinetic and pharmacodynamic models. Absorption into the cornea and conjunctiva is usually described by a first-order process but the corneal permeation profile may not be always a first-order process. It depends on the formulation design of the delivery system.

A constant activity delivery system may not exhibit a steady-state penetration process through a biomembrane[5]. An earlier study of amount of butylparaben permeation through guinea pig skin has shown an initial curved stage and then becomes a linear in the latter stage. The initial stage of permeation is called non-steady state condition while in the latter stage, the rate of permeation is constant and the system is called as steady state[6].

Development of predictive capability of the event like molecular mass transport across the biological membranes demands keen analysis of its kinetics involved. The drug transport kinetics is influenced by the parameters like drug type, polymorphic form, crystallinity, particle size, solubility and the permeation enhancers in the dosage form[7,8]. Drug transport kinetics as

realized by mathematical models could have utmost significance with respect to optimization of formulations[9]. Andrés-Guerrero et al built a kinetic ocular model was, in order to predict dexamethasone concentrations in the rabbit eye[10]. In the past many investigators[11-17] have tested several mathematical models and semi-empirical equation including First-order, Higuchi, and Korsmeyer-Peppas models for model fitting purpose. First order kinetics of drug diffusion is concentration dependent and decrease exponentially with time. Higuchi model diffusion pattern from heterogeneous matrix system is directly proportional to the square root of time and involves tourtuosity, which leads to Fickian diffusion. Korsmeyer–Peppas model, a semi empirical equation relates exponential diffusion of drug to the elapsed time. According to Fick's law, mass transfer across a bio-membrane is the reflection of the magnitude of concentration gradient. Flux of eluting species mainly depends on the thermodynamic drag created by the gradient difference between donor and receiver compartment. The whole phenomenon involving dissolution of drug molecule, followed by permeation of the dissolved species is the outcome of two individual steps such as non-steady state and steady state[18-20]. Lag time is the predetermined time difference between the time of drug entry into the bio-barrier (non-steady state diffusion) and reach out latter for the steady state[21,22].

It has been established by several researchers that drug transit is a stochastic phenomenon where cluster of active therapeutic agent is targeted to the specific biological site of action due to the chance of random scatter[23,24]. Moment analysis is a preferred tool in the quiver of statistics for quantification of parameters in biological system. In chemical engineering statistical moment analysis has been employed for the depiction of diffusional behavior of chemical entities in liquid[25] and diffusion in a tube[26]. Statistical moment analysis, being a non-compartmental approach is well accepted in pharma sector as it permits a comprehensive pharmacokinetic

analysis without resort to curve-fitting, computes, or tedious mathematical equations. Many pharmacokinetic parameters of prime significance such as volume of distribution, mean residence time, clearance and bioavailability can be estimated using statistical moment analysis without the complicated non-linear regression approach of compartmental analysis[27-29]. Previously, numerous explorations were conceded to characterize corneal permeability mechanism and predicted drug delivery rates to the eye[30,31]. Previously several models have been examined to explain drug transport kinetics[32,33] and many investigators have characterized in vitro and in vivo correlation employing statistical moment analysis[34-36]. Conventional model analysis is the usually applied tool in describing the bio-membrane permeation kinetics[37].

The present report has described the mechanism of corneal permeation kinetics of diclofenac potassium (DCP) hydrogel film[38] formulation incorporating with triethanolamine (TRE) as plasticizer using conventional mathematical models and statistical moment theory. Mean residence time for non-steady state (MRT_N), mean residence time for steady state (MRT_S) and mean residence time for permeation (MRT_P) were determined statistically by the moment analysis of permeation data. The extent of permeation in non-steady state (EPN), extent of permeation in lag time (EPL), extent of permeation in steady state (EPS) and total amount permeated in 360 min (TAP) were quantified. The surface morphology was explored by scanning electron microscopy (SEM). The crystallinity study was done by x-ray diffractometry (XRD). Coefficient of determination (r^2) and standard error of estimate (SEE) were evaluated for establishment of Level "A" correlation between in-vitro dissolution and ex-vivo steady state permeation at each time point. DCP-HPMC binding configuration was generated using docking calculation to study drug-excipient interactionat molecular level. Extensive literature review revealed that this type of characterization has very rarely been performed earlier.

2. Materials and Methods

2.1 Materials

The active compound diclofenac potassium was purchased from Tejani Life care, Cuttack, India and hydroxypropyl methylcellulose (HPMC K15 M) and carrageenan were procured from Himedia Laboratories Pvt. Ltd, India. Triethanolamine was obtained from Merck Ltd, Mumbai, India. All other chemicals were of reagent grades as required.

2.2 Fabrication of hydrogel film for corneal permeation

Hydrogel films containing DCP in HPMC matrix were formulated by casting and solvent evaporation method[39-41]. Accurately weighed DCP and TRE were dissolved in ethanol and added to the previously prepared homogeneous dispersion gel of HPMC under stirring. The obtained clear hydrogel mass was poured to petri dish (Tarsons, diameter: 90 mm) and dried at 40 °C until constant weight. Formulated casting film is composed of DCP (376 mg) and HPMC (1133 mg) including TRE as plasticizer 0, 10, 20, or 30 % wt/wt of polymer and the thickness of the film was measured at six points using micrometer gauze (Mitutoyo, Japan).

2.3 In-vitro drug release study

In-vitro release study was carried out in 200 ml phosphate buffered saline, pH 7.4 as dissolution medium for 6 h using USP type II apparatus (Electrolab, dissolution tester USP, TDT06L, India). Many reports are available where phosphate buffered saline (pH 7.4, 200 ml) has been used as dissolution medium for in-vitro dissolution study of ocular formulations using USP type II dissolution apparatus to simulate tear fluid[42-45]. The United States Pharmacopeia also states: “When sink conditions are present, it is more likely that dissolution results will reflect the properties of the dosage form”. Accurately weighed strip of each film was cut and adhered to the glass slide with cyanoacrylate adhesive and placed inside the dissolution vessel. The dissolution

was carried out at 34.0 ± 0.5 °C at agitation rate 50 rpm. Aliquots of media were withdrawn at predetermined time through 0.45 µm membrane filter and analyzed spectrophotometrically at 276 nm in triplicate.

2.4. Ex-vivo corneal permeation study

Fresh sheep eyes were collected from slaughter house within 1 h of its sacrifice. The cornea with attached 5-6 mm wide scleral ring was excised from the whole eye. After applying a properly cut piece of film on the center, the dissected cornea was mounted in the diffusion cell apparatus[46]. The corneal epithelium was placed facing the donor compartment vertically with an effective area of 1.43 cm^2 and the diffusion media (phosphate buffered saline, pH 7.4) was placed in the receptor compartment. The diffusion was continued for 6 h at 34 °C under constant stirring in triplicate. Withdrawn samples (10 ml) at regular intervals were filtered through a 0.45 µm membrane filter and recorded at 276 nm using UV–VIS spectrophotometer (JASCO V-630 spectrophotometer, Software: Spectra Manager).

2.5 Permeation kinetics and statistical moment analysis

Permeation kinetics through corneal tissue was evaluated using various mathematical models like first order, Higuchi, and Korsmeyer–Peppas model equations[12]. The lag time of permeation, time required up to 50 % permeation, permeation rate constant, permeation exponent (n) and coefficient of determination (r^2) were estimated as per model regression equation. Further, estimated lag time of permeation, time required up to 50 % permeation, permeation rate constant and permeation flux for steady state were also calculated from the x-intercept of the linear region of corneal permeation profile using regression analysis[47].

Mean residence time for non-steady state (MRT_N), mean residence time for steady state (MRT_S) and mean residence time for permeation (MRT_P) were determined statistically by the

moment analysis of permeation data. The extent of permeation in non-steady state (EPN), extent of permeation in lag time (EPL), extent of permeation in steady state (EPS) and total amount permeated in 360 min (TAP) were quantified. The highest Non-steady state and steady state parameters were elucidated from permeation profile according to Fick's law of diffusion. Following relations were employed for elucidation of MRT_N, MRT_S and MRT_P using the first moment of amount of drug permeated *vs.* time curve.

$$MRT_N = AUMC_{(0 - 120)} / AUC_{(0\text{-}120)} \quad \text{--------- (1)}$$

$$MRT_S = AUMC_{(120 - 360)} / AUC_{(120\text{-}360)} \quad \text{--------- (2)}$$

$$MRT_P = AUMC_{(0 - 360)} / AUC_{(0 - 360)} \quad \text{--------- (3)}$$

Where, AUMC is the area under the product of amount permeated and time (the first moment AUC) versus time curve. $AUMC_{(0 - 120)}$ was calculated from initial sampling time to sampling at 120 min and $AUMC_{(120–360)}$ was derived from 120 min to last sampling time employing MATLAB 7.0 software. $AUMC_{(0 - 360)}$ is the summation of $AUMC_{(0 - 120)}$ and $AUMC_{(120 - 360)}$. Extent of permeation in non-steady state (EPN), extent of permeation in lag time (EPL), extent of permeation in steady state (EPS) andtotal amount permeated up to 360 min (TAP) were evaluated from the amount permeation vs. time profile to understand the effect of TRE on permeation threshold of the films.

One way analysis of variance (ANOVA) was applied to compare the effect of formulation variable on different steady and non steady state parameters such as EPN, EPL, EPS and TAP employing XLSTAT software[48]. Two sided Dunnett's test was performed for pair wise comparison with the control (L1 containing 0 % plasticizer) as L1 *vs*. L2 (10 % plasticizer), L1 vs L3 (20 % plasticizer) and L1 vs L4 (30 % plasticizer).

Level "A" correlation between in-vitro dissolution and ex-vivo steady state permeation at each time point has been determined. The accuracy of predictions has been made with the regression line by determining standard error of estimate (SEE) which measures unexplained variation. Coefficient of determination (r^2) and standard error of estimate (SEE) were evaluated for establishment of Level "A" correlation between in-vitro dissolution and ex-vivo steady state permeation at each time point.

2.6 Surface morphology and crystallinity of the film

Surface morphology of the films was investigated using Scanning electron microscope (JSM- 6390, JEOL, Tokyo, Japan). Prior to imaging the dried samples were mounted on metal stab for gold coating under applied vacuum. The photomicrographs were taken at different magnifications employing electron imaging operating at an accelerated voltage of 10 kV.The XRD pattern of pure diclofenac and the films were recorded using X-Ray diffractometer (Model: Philips analytical X-Ray with PC-APD, Diffraction Software). The voltage and current were 40 kv and 15 mA, respectively. Anode Material Cu, K-Alpha (radiation 1.5406 Å) was used as a source of X-rays. Measurements were undertaken at a scan speed of 1 °/min for the scanning angle ranging from 10 ° to 60 ° (2θ). Differential scanning calorimetry (Universal V4.2E TA Instruments) was employed to analyze the thermal behavior and crystalinity of the pure drug and formulated films. Samples (about 2-3 mg) were weighed into an aluminum pan and scanning was carried out at a rate of 10 °C/min at temperatures between 30 °C and 330 °C, using a nitrogen gas purge at 50 ml/min.

2.7 Conjunctival anti-inflammatory study

New Zealand albino male rabbits (three animals) weighing about 3 to 3.2 kg were employed for the conjunctival anti-inflammatory study. Approval for the use of animals in this

study was obtained from the SOA University Animal Ethics Committee (SOA University, Odisha, India, Reg. no.1171/C/08/CPCSEA). The inflammation was induced by subconjuctival injection of carrageenan. Prior to induction of inflammation the eye of the animal was anesthetized by Proparacaine Hydrochloride Ophthalmic Solution USP 0.5 %. Then carrageenan (200 µl, 3 % saline solution) was injected into the upper palpebral region of the anesthetized eye[49]. Micro syringe (Dispo van 30G, India) fitted with 30 gauge needle was used to serve the purpose. One hour after carrageenan injection when inflammation was induced to the marked extent a small piece of the film (L4, about 3 mm/1.5 mm) was placed in the cul-de-sac and the anti inflammatory activity of the film has been recorded.

2.8 Conformational analysis by molecular modeling

In the film formulation diclofenac molecule remained in dispersed state in the HPMC matrix. The computer-aided molecular modeling approach was used for conformational analysis of drug–polymer complexation during dispersions. The molecular structures of drug and polymer were drawn and 3D molecular models were generated using MARVIN DRAW software (ChemAxon, Budapest, Europe). The drug–polymer complex was architecturally prepared by docking in the software AUTODOCK VINA[50]. Further processing and visualization was performed in Open Babel 2.3.1 and Discovery studio 3.5 (Accelrys) software respectively. Only one repeat unit of HPMC was built for interaction due to the following reasons: (a) one repeat unit contained alldifferent atom groups, (b) the calculation ofa single repeat unit was economical[51].

3. Results and Discussion

3.1 Kinetics of permeation

All the formulated films (L1, L2, L3 and L4) have shown uniform thickness (244 ± 9, 245 ± 4, 242 ± 6 and 246 ± 5 μ respectively). Dissolution profile of diclofenac film formulations (Figure 1) showed a steady increase in drug release with the increase in triethanolamine content in the film. When compared with the control film without TRE (L1), the film L2, L3 and L4 demonstrated a gradual increase in drug release. Figure 2 depicts the amount of drug permeated from formulated films at 34 °C as a function of time. An increasing trend of amount permeation was observed with increasing TRE content inpresence of HPMC. Amount permeation of different formulations was found in the following order as: L1 (control) < L2 < L3 < F4. Several mathematical models such as First order, Higuchi and Korsmeyer-Peppas model were examined for kinetic modeling of permeation data of diclofenac hydrogel formulation and data was tabulated in Table 1. After model fitting as per First order (r^2 values 0.955 to 0.986) and Higuchi model (r^2 values 0.916 to 0.970) estimated lag time of permeation ($t_{f,lag}$, and $t_{h,lag}$ respectively) was evaluated and reported in Table 1. Also depicted the estimated time required up to 50 % permeation ($t_{f,50\%}$, $t_{h,50\%}$, and $t_{kp,50\%}$) as per First order, Higuchi and Korsmeyer-Peppas (r^2 values 0.967 to 0.990) equation respectively. k_f and k_h are the calculated permeation rate constant as per First order and Higuchi equation respectively. Permeation exponent estimated from Korsmeyer-Peppas equation (n values 2.16 to 2.93) indicates that permeation mechanism of all the hydrogel films are fully under diffusion control. Kinetic modeling of permeation data clearly confirmed the positive influence on the permeation as TRE increased in the formulation.

It has been cleared from literature that though the permeation follows Korsmeyer-Peppas model kinetics, its rate is not only limited to drug diffusion but also to the factors like polymeric chain relaxation[52] affected by plasticizer and surfactant effect by preservative. TRE as plasticizer, played important role in polymeric chain relaxation and flexibility and permitted easy ingress of

drug molecule. Permeation of drug through a bio-membrane conventionally can be characterized by non steady state and steady state. Lag time is the transient component of permeation process, achieved from fixed time differentiation monitored between the time of corneal drug entry and the time at which the permeation rate reaches a steady state. The lag time ($t_{ss,lag}$) was estimated from the *x*-intercept of the linear region of permeation profile using regression analysis. Steady state permeation parameters of the film formulations are reported in Table 2. It was evident that the value of the lag time has been tagged on to a paradigm with respect to plasticizer concentration. Gradual reduction in $t_{ss,lag}$ was observed as the plasticizer concentration increased. Triethanolamine, a hydrophilic plasticizer containing hydroxyl and amino functions in the film formulation decreased the lag time of permeation from 29.4 to 17.4 min when its concentration was varied from 0 to 30 %. Fundamental relationship of Fick's first law used in the pharmaceutical diffusion process was applied for the estimation of $t_{ss50\%}$, steady state rate constant (k_{ss}) and permeation flux (J_{ss}). Parameters indicating improved permeation ($t_{ss50\%}$, values 459.6 to 345.0 *min*; *kss* values 0.134 to 0.151 $\mu g.min^{-1}$ and J_{ss} values 4.55 to 5.70 $\mu g.cm^{-2}.min^{-1}$) were also resulted by the increased content of TRE in the film formulation. Since water, butanol, and glycerol are very small molecule and high hydrophilic compounds their permeability across the intact cornea is significantly larger[53] than that of lomefloxacin hydrochloride and dexamethasone. Yasueda et al., (2007) performed diffusion experiment through rabbit intact cornea with test solution of 0.3% lomefloxacin hydrochloride (hydrophilic drug) in 2.6% glycerine (pH 5.0) and 0.008% dexamethasone (hydrophobic drug) in receptor buffer of pH 7.2 and flux value was found to be 0.011 and 0.1368 $\mu g.cm^{-2}.min^{-1}$ respectively[54]. They have also estimated the lag time of permeation as 48 and 60 min respectively. The results of present investigation have revealed the significant improvement of ocular permeability DCP.

Permeation parameters MRT_N, MRT_S and MRT_P were estimated by the statistical moment analysis and depicted in Table 3. Increase in TRE from 0 to30 % lowered the MRT_N from 106.2 to 94.2 min. Analogous reduction pattern in MRT_S (273.6 to 261.0 min) and MRT_P (269.4 to 248.4 min) was followed with the increase in TRE. Increased loading of TRE acted as the permeation booster and improved permeation by breaking the physiological barriers of the corneal tissue. Films with lower plasticizer concentration possessed higher retention values as a sign of permeation retardation. Extent of permeation in non-steady state (EPN), extent of permeation in lag time (EPL), extent of permeation in steady state (EPS) and total amount permeated in 360 min (TAP) were evaluated from the amount permeation *vs.* time profile (Table 3) to understand the effect of TRE on permeation threshold of the films.

Fisher's F test was used here and the probability corresponding to the F values in the cases of all parameters are 0.0001. It means that we would take a 0.01% risk to conclude that the null hypothesis (no effect of the film formulation variable) is wrong. So it can be concluded with confidence that there is an effect of the film formulation on the magnitude of parameters. It also can be noted that the *r* values corresponding to different parameters are good (0.991, 0.997, 0.956 and 0.992). This means all the information offering a complementary explanation of the variations of the parameters that has been established. Further, Dunnett's test revealed that all the formulations are significantly different from the control (L1 containing 0 % plasticizer) when comparison was made pair wise with the control as L1 vs L2 (10 % plasticizer), L1 vs L3 (20 % plasticizer) and L1 vs L4 (30 % plasticizer) with less than 0.09 % risk (Table 4.). Influence of TRE in the film (L1, L2, L3 and L4) on corneal permeation EPN, EPL, EPS and TAP has been shown in Figure 3. Means chart of observed and predicted EPN, EPL, EPS and TAP of four formulations has also been presented in Figure 4 to understand the limit of prediction.

The correlation coefficient and regression equation of in-vitro dissolution and steady state ex-vivo permeation (Figure 5) have been tabulated in Table 5. In the present study correlation coefficient (0.9803 – 0.9990) of in-vitro dissolution and steadystate ex-vivo permeation of the films indicated a good Level "A" correlation-ship between them. The good correlation-ship indicated batch to batch consistency in the ex-vivo performance of the films by the use of such in vitro values.

3.2 Characterization of hydrogel film

Photomicrograph of pure DCP contains distinct compact drug crystals in micron scale (Figure 6). All the films were microporous and of uniform surface morphology due to homogeneous mixing of dug crystal in the polymer matrix of HPMC. Here, HPMC played a keyrole as drug crystal growth inhibitor and a habit modifier[55]. Keen observation demonstrated that film without plasticizer (L1) presented a relatively irregular, rigid, packed and porous surface with embedded minute drug crystals. Films with plasticizer and preservatives exhibited a smoother and continuous surface (L2, L3 and L4). Crystals grown in the film in presence of TRE were found smaller than the crystals grown without TRE. The XRD spectra and DSC thermograms of the diclofenac potassium and drug loaded polymeric films were portrayed in Figure 7 (a,b). The characteristic peaks appearing at 13.25, 20.40, 21.07, 25.24, 26.17, 30.15 and 26.82 2θ values in the XRD pattern of diclofenac potassium clearly revealed the crystalline nature of the drug. The increase of the full width at half maximum (FWHM) of all the films with respect to DCP supported molecular dispersion of pure drug and polymer. Reduced intensity signals of L1 (without TRE) were attributable to the partial amorphization of the drug under the influence of HPMC only. The absence of prominent peaks in the diffractogram of other film formulations (L2, L3 andL4) confirmed the existence of the drug in microcrystalline form in the

polymer matrix. It may be inferred from the study that a major portion of the drug incorporated existed as solid-solid solution in the polymer matrix where as the small remaining fraction has been crystallized in the microcrystalline and amorphous form in the polymeric matrices. The exothermic peak at 313.2 °C in DSC thermogram of pure drug is the outcome of drug decomposition without melting[56]. In the films no endothermal or exothermal peaks for DCP are observed near 313.2 °C. This is possibly due to the transformation of drug from crystalline to amorphous or microcrystalline state. The molecular dispersion of diclofenac in polymeric matrix of HPMC is seemed to be protecting the drug from decomposition by formation of hydrogen bonding forming with the drug. Each film exhibited similar thermal behavior. The wide endothermic peaks at 70 to 100 °C correspond to moisture loss from HPMC in the films[57-59].The glass transition temperature can be used as a measurement for the mobility of the macromolecules and also give information about the molecular mobility of the drug and changes at its semi–crystalline state. Glass transition of DCP in the films was manifested through a small step-like formation in the range of 210 to 219 °C. DSC thermogram of 6-mercaptopurine-HPMC granules prepared by wet granulation technique showed a markedly reduced intensity of endothermic peak of drug indicating amorphization of drug[60]. Panda et al[59] reported the disappearance of melting endotherm in the DSC thermogram of HPMC matrix film containing telmisartan suggesting possible molecular dispersion of drug in polymeric matrix. A decrease in the melting endothermic onset and a reduction of the melting enthalpy of diclofenac were reported in the DSC thermogram of diclofenac and HPMC physical mixture (1:1) suggesting a probable eutectic formation between drug and polymer[61].

3.3 Conjunctival anti-inflammatory study

Figure 8 (a-g) summarizes the stages of anti inflammatory study conducted. Signs of inflammation such as conjunctival swelling and redness were visible after one hour of the carrageenan injection and intensity of symptoms were increased gradually there after. Figure 8 (a) shows the carrageenan injection to upper palpebral region of eye. Normal rabbit eye before injection and inflammatory condition of the eye after 1 hour of injection (acute inflammation) have been shown in Figure 8 (b) and (c) respectively. Figure 8 (d) shows the film just after applying in the eye. After 1 hour of film application inflammation has been subsided partially and the film has been partially swelled and eroded (Figure 8e). Two hour after film application inflammation subsided almost fully and residual film was left (Figure 8f). Film dimension used for the study has presented in Figure 8g.

3.4 Conformational analysis by molecular modeling

Docking can explore the fitting of two molecules with a stable configuration and a favorable energy. The docked complexes of Diclofenac with HPMC were selected in terms of the free energy of binding andthe statistic information of the population of the complexes. The free energy of binding included intermolecular energy (vander Waals, H-bonding interactions, desolvation, and electrostatic energies) and torsional free energy. An advantage of this docking is that it supplies not only the possible physical interactions but also the possible complex configuration. Figure 9*a* and 9*b* portrays the protein data bank structure of DCP and HPMC respectively. The study revealed that a definitive energy minimization was possible for drug and drug–polymer complex. The best docked DCP-HPMC (Figure 9*c*) complex had a binding energy of −2.5 kcal/mol. It has been confirmed that there is the possibility for formation of a complex between drug and polymer as evident from the energy-minimized structure of the drug–polymer complex. The drug molecule was able to bind with polymer at the free alkyl groups by formation

of hydrogen bonding. The negative docking energy of the complex formation corresponds with solubility enhancement leading to a more stable nature of the drug–polymer complex.

4. Conclusions

Kinetic modeling of corneal permeation data using conventional First order, Higuchi and Korsmeyer-Peppas equation clearly confirmed the positive influence on the permeation as TRE increased in the hydrogel films formulation. Statistical moment analysis could be utilized successfully for estimation of non steady state and steady state corneal permeation parameters MRTN, MRTS and MRTP. Highly improved values of EPN, EPL, EPS and TAP of the hydrogel formulations were observed when compared with the control film. Level "A" correlation between in-vitro dissolution and ex-vivo steady state permeation has been established to ensure batch-to-batch consistency in the biological performance of diclofenac potassium. Hydrogel formulation characterization by SEM and XRD suggested the inhibition of the crystal growth and partial amorphisation of diclofenac in the film. Anti inflammatory activity has been noticed after application of the hydrogel film distinctly. DCP-HPMC interaction at molecular level has been confirmed using binding configuration and docking calculation.

Conflicts of Interest

Authors declare no conflicts of interest.

Acknowledgements

The authors are acknowledging gratefulness to the Department of Science & Technology, Ministry of Science & Technology, New Delhi, India, for providing INSPIRE fellowship to Mr. Rajaram Mohapatra (IF 10199). The authors are also very much thankful to Prof. Manoj Ranjan Nayak, President, Siksha O Anusandhan University for providing other facilities and

encouragement. Authors are also grateful to the editor and anonymous reviewers for their valuable comments and suggestions.

References

1. P. W. J. Morrison, C. J. Connon and V. V. Khutoryanskiy, *Mol. Pharmaceutics,* 2013, **10**, 756–762.
2. V. V. Khutoryanskiy, Mucoadhesive materials and drug delivery systems, John wiley & Sons Ltd, London, 2014.
3. K. J. Himmelstein, I. Guvenir and T. F. Patton, *J. Pharm. Sci.,* 1978, **67**, 603–606.
4. S. C. Miller, K. J. Himmelstein and T. F. Patton, *J. Pharmacokinet. Biopharm.* 1981, **9**, 653–677.
5. S. Pattnaik, K. Swain, J. V. Rao, V. Talla, K. B. Prusty and S. K.S ubudhi, *RSC Adv.,* 2015, **5**, 74720-74725
6. H. Komatsu and M Suzuki, *J. Pharm. Sci.,* 1979, **68**, 596–598.
7. Tojo K, *Chem. Pharm. Bull.* 2004, **52**, 1290–1294.
8. S. Pattnaik, K. Swain, J. V. Rao, V. Talla, K. B. Prusty and S. K. Subudhi, *RSC Adv.,* 2015, **5**, 91960-91965
9. S. Dash, P. N. Murthy, L. Nath and P. Chowdhury, *Acta Pol. Pharm. Drug* Res., 2010, **67**, 217-223.
10. V. Andrés-Guerrero, M. Zong, E. Ramsay, B. Rojas, S. Sarkhel, B. Gallego, R. de Hoz, Ramírez AI, J. J. Salazar, A. Triviño, J. M. Ramírez, E. M. Del Amo, N. Cameron, B. de-Las-Heras, A. Urtti, G. Mihov, A. Dias and R. Herrero-Vanrell. *J. Control. Rel.,* 2015, **211**, 105–117.

11. S. A. Abdel-Hameed, A. M. El-Kady and M. A. Marzouk, *Mater. Sci. Eng. C Mater. Biol. Appl*., 2014, **44**, 293-309.
12. A. Hadjitheodorou and K. George, *Mater. Sci. Eng. C* 2014, **42**, 681–690.
13. S. Mallick, B. K. Gupta and S. K. Ghoshal, *Acta Pol. Pharm. Drug Res.,* 1999, **56**, 289-295.
14. S. Mallick, B. K. Gupta and S. K. Ghoshal, *J. Sci. Ind. Res.,* 1999, **58**, 1010-1016.
15. S. Mallick, A. Sahu and K. Pal, *Acta Pol. Pharm. Drug Res*., 2004, **61**, 21-30.
16. D. Ramyadevi and K. S. Rajan, *RSC Adv.,* 2015, **5**, 12956-12973.
17. É. A. Estracanholli, F. S. G. Praça, A. B Cintra, M. B. Pierre and M. G. Lara, *AAPS PharmSciTech,* 2014, **15**, 1468-1475.
18. R. J. Scheuplein, *J. Invest. Dermatol.* 1967, **48**, 79-88.
19. S. Mallick, S. Pattnaik, Swain K and P. K. De, *Drug Dev. Ind. Pharm.,* 2007, **33**, 865-873.
20. S. Pattnaik, K. Swain, P. Choudhury, P. K. Acharya and S. Mallick, *Int. Braz. J. Urol.,* 2009, **35**, 716-729.
21. H. Tang, D. Blankschtein and R. Langer, *J. Pharm. Sci.,* 2002, **91**, 1891-1907.
22. R. Ash, *J. Membr. Sci.,* 1996, **117**, 79-108.
23. S. Riegelman and P. Collier, *J. Pharmacokinet. Biopharm.,* 1980, **8**, 509-534.
24. K. Yamaoka, T. Nakagawa and T. Uno, *J. Pharmacokinet. Biopharm.,* 1978, **6**, 547-558.
25. Y. Kwon, Handbook of Essential Pharmacokinetics, Pharmacodynamics and Drug Metabolism for Industrial Scientists, 9th ed. Springer press, New York, 2002.
26. R. Aris, *Proc. Roy. Soc.* 1956, **235**, 67–77.
27. Y. I. Kim, R. Pradhan, B. K. Paudel, J. Y. Choi, H. T. Im and J. O. Kim, *Arch. Pharm. Res.,* 2015, **38**, 2163-2171.

28. S. Mallick, B. K. Gupta and S. K. Ghosal, *Acta Pol. Pharm. Drug Res.,* 2000, **57**, 175-180.

29. S. Mallick, B. K. Gupta and S. K. Ghosal. *Indian J. Pharm. Sci.,* 2000, **62**, 303-306.

30. M Ahuja and D. C. Bhatt, RSC *Adv.,* 2015, **5**, 82363-82373.

31. L. R. Schopf, A. M. Popov, E. M. Enlow, J. L. Bourassa, W. Z. Ong, P. Nowak and H. Chen, *Transl. Vis. Sci. Technol.,* 2015, **4**, 1-12.

32. L. R. Schopf, E. Enlow, A. Popov, J. L. Bourassa and H. Chen, *Ophthalmol. Ther.,* 2014, **3**, 63-72.

33. M. J. Coffey, H. H. Decory, S. S. Lane, *Clin. Ophthalmol.,* 2013, **7**, 299-312.

34. S. Yamamura, F. Aida, Y. Momose and E. Fukuoka, *Drug Dev. Ind. Pharm.,* 2000, **26**, 1-6.

35. G. Schliecker, C. Schmidt, S. Fuchs, E. Ehinger, J. Sandow and T. Kissel, *J. Control. Rel.,* 2004, **94**, 25-37.

36. G. C. Athanassiou, D. M. Rekkas and N. H. Choulis, *Int. J. Pharm.,* 1993, **90**, 51-58.

37. A. Pedacchia and A. Adrover, C*hem. Eng. Res. Des.,* 2014, **92**, 2550–2556.

38. D. Das and S. Pal, *RSC Adv.,* 2015, **5**, 25014-25050.

39. K. Swain, S. Pattnaik and S. Mallick. *J. Drug Target.,* 2010, **18**, 106-114.

40. K. Swain, S. Pattnaik, S. C. Sahu, S. Mallick, *Lat. Am. J. Pharm.,* 2009, **28**,706-714.

41. S. Pattnaik, K. Swain, Bindhani A, S. Mallick, *Drug Dev. Ind. Pharm.,* 2011, **37**, 465-474.

42. M. Al-Ghabeish, X. Xu, Y. S. Krishnaiah, Z. Rahman, Y Yang and M. A. Khan, *Int. J. Pharm*., 2015, **495** 783–791.

43. P. B. Deshpande, P. Dandagi, N. Udupa, S.V. Gopal, S. S. Jain and S. G. Vasanth, *Pharm. Dev. Technol*., 2010, **15**, 369–378

44. X. Xu, M. Al-Ghabeish, Z. Rahman, Y. S. Krishnaiah, F. Yerlikaya, Y. Yang, P. Manda, R. L. Hunt and M. A. Khan, *Int. J. Pharm*., 2015, **493,** 412–425.

45. H. Kao, H. Lin, Y. Lo and S. Yu, *J. Pharm. Pharmacol*., 2006, **58**, 179–186.

46. M Rodriguez-Aller, D Guillarme, ME Sanharawi, F. Behhar-Cohen. J. L. Veuthey and R. Gurny, *J. Control. Rel*., 2013, **170**, 153–159.

47. S. D. Palma, L. I. Tartara, D. Quinteros, D. A. Allemandi, M. R. Longhi and G. E. Granero, *J. Control. Rel.,* 2009, **138**, 24–31.

48. https://help.xlstat.com/customer/en/portal/articles/2062232runningaonewayanovafollowedbymultiplecomparisonstestswithxlstat?b_id=9283

49. M. Kato, Y. Hagiwara, T. Oda, M. Imamura-Takai, H. Aono and M. Nakamura, *J. Ocul. Pharmacol. Therapeut.,* 2011, **27**, 353-360.

50. O. Trott and A. J. Olson, *J. Comput. Chem.,* 2010, **31**, 455-461.

51. C. Li, J. X. Wang, Y. Le and J. F. Chen, *Mol. Pharmaceutics,* 2013, **10**, 2362−2369.

52. M. G. A. Vieira, M. A. Silva, L. O. Santos, M. M. Beppu, *Eur. Polym.,* 2011, **47**, 254-263.

53. G. M. Grass and J. R. Robinson, *J. Pharmaceut., Sci.,* 1988, **77**, 3–14.

54. S. Yasueda, M. Higashiyama, M. Yamaguchi, A. Isowaki and A. Ohtori, *Drug Dev. Ind. Pharm*., 2007, **33**, 805-811.

55. S. L. Raghavan, A. Trividic, A. F. Davis, J. Hadgraft, *Int. J. Pharm.,* 2001, **212**, 213–221.

56. A. Fini, M. Garuti, G. Fazio, J. Alvarez-Fuentes and M. A. Holgado, *J. Pharm. Sci.,* 2001, **90**, 2049–2057.

57. J. L. Ford, *Int. J. Pharm*., 1999, **179**, 209–228.

58. L. Perioli, V. Ambrogi, C. Pagano, E. Massetti and C. Rossi, *Colloids Surf. B: Biointerfaces,* 2011, **84**, 413–420.

59. B. Panda, A. S. Parihar, S. Mallick, *Int. J. Biol. Macromol*., 2014, **67**, 295–302.

60. R Chowdhary, R S Pai, G Singh., *Int J Pharm Invest*., 2013, **3**, 217-224.

61. M. L. Vueba, L. A. E. B. Carvalho and M. E. Pina, African J. Pharm. Pharmacol. 2013, 7, 83-97.

Table 1. Kinetic modeling of permeation data of diclofenac film formulation

Film code	First order				Higuchi				Korsmeyer-Peppas		
	$t_{f,lag}$ (min)	$t_{f,50\%}$ (min)	k_f (min^{-1})	r^2	$t_{h,lag}$ (min)	$t_{h,50\%}$ (min)	k_h ($\%rel^{-1/2}$)	r^2	$t_{kp,50\%}$ (min)	n	r^2
L1	53.0	579.6	0.0013	0.955	57.0	199.2	0.356	0.916	340.2	2.93	0.990
L2	39.9	493.8	0.0016	0.986	37.8	176.4	0.389	0.945	315.0	2.16	0.967
L3	37.4	450.6	0.0017	0.967	36.6	169.8	0.407	0.947	276.6	2.50	0.982
L4	31.7	387.6	0.0025	0.974	32.4	139.8	0.521	0.970	226.8	2.17	0.980

$t_{f,lag}$, and $t_{h,lag}$ are the estimated lag time of permeation as per First order and Higuchi model respectively; $t_{f,50\%}$, $t_{h,50\%}$, and $t_{kp,50\%}$ are the estimated time required up to 50 % permeation as per First order, Higuchi and Korsmeyer-Peppas equation respectively; k_f and k_h are the calculated permeation rate constant as per First order and Higuchi equation respectively; n is the permeation exponent estimated from Korsmeyer-Peppas equation.

Table 2. Corneal permeation parameters for steady state

Film code	$t_{ss,lag}$ (*min*)	$t_{ss,50\%}$ (*min*)	k_{ss} ($\mu g.min^{-1}$)	J_{ss} ($\mu g.cm^{-2}.min^{-1}$)	r^2
L1	29.4	459.6	0.134	4.55	0.994
L2	21.6	379.2	0.136	5.15	0.992
L3	19.2	366.6	0.146	5.34	0.965
L4	17.4	345.0	0.151	5.70	0.990

$t_{ss,lag}$, $t_{ss,50\%}$, k_{ss} and J_{ss} are the estimated lag time of permeation, time required up to 50 % permeation, permeation rate constant and permeation flux for steady state respectively.

Table 3. Steady state and non-steady state corneal permeation parameter using statistical moment analysis

Film code	MRT_N (min)	MRT_S (min)	MRT_P (min)	EPN (*μg*)	EPL (*μg*)	EPS (*μg*)	TAP (*μg*)
L1	106.2 ± 8.23	273.6 ± 31.57	269.4 ± 12.53	228.0 ± 5.86	2.12 ± 0.12	1555.0 ± 13.58	1783.0 ± 26.83
L2	100.2 ± 11.53	267.0 ± 31.45	259.2 ± 8.03	493.0 ± 5.39	4.36 ± 0.47	1769.0 ± 17.35	2262.0 ± 24.39
L3	99.6 ± 24.12	265.2 ± 5.78	256.8 ± 14.31	669.0 ± 14.11	12.13 ± 0.26	1951.0 ± 7.59	2620.0 ± 13.48
L4	94.2 ± 7.02	261.0 ± 13.75	248.4 ± 7.53	727.0 ± 12.82	14.95 ± 1.47	1980.0 ± 22.11	2707.0 ± 53.34

MRT_N= Mean residence time for non-steady state
MRT_S= Mean residence time for steady state
MRT_P= Mean residence time for permeation
EPN= Extent of permeation in non-steady state
EPL= Extent of permeation in lag time
EPS= Extent of permeation in steady state
TAP= Total amount permeated in 360 *min*

Table 4.Dunnett two sided analysis of the differences between the control category L1 and the other catagories with a confidence interval of 95%.

	Category	Difference	Standardized difference	Critical value	Critical difference	Pr > Diff	Significant
EPN	L1 vs L4	-499.333	-27.338	2.880	52.598	0.00001	Yes
	L1 vs L3	-441.000	-24.145	2.880	52.598	0.00001	Yes
	L1 vs L2	-265.333	-14.527	2.880	52.598	0.00001	Yes
EPL	L1 vs L4	-12.823	-46.667	2.880	0.791	0.00001	Yes
	L1 vs L3	-10.003	-36.405	2.880	0.791	0.00001	Yes
	L1 vs L2	-2.233	-8.128	2.880	0.791	0.00001	Yes
EPS	L1 vs L4	-425.000	-11.694	2.880	104.663	0.00001	Yes
	L1 vs L3	-396.333	-10.905	2.880	104.663	0.00001	Yes
	L1 vs L2	-214.333	-5.897	2.880	104.663	0.0009	Yes
TAP	L1 vs L4	-923.667	-27.500	2.880	96.723	0.00001	Yes
	L1 vs L3	-836.667	-24.910	2.880	96.723	0.00001	Yes
	L1 vs L2	-479.000	-14.261	2.880	96.723	0.00001	Yes

Table 5. Level "A" correlation between in-vitro dissolution and ex-vivo steady state permeation

Film code	*r*	Regression equation	Coefficient of non-determination (%)[a]	Standard error of estimate
L1	0.9930	$y = 1.606x - 5120$	1.4	0.0683
L2	0.9808	$y = 1.981x - 6984$	3.8	0.1125
L3	0.9990	$y = 1.997x - 6395$	2.0	0.0258
L4	0.9803	$y = 2.052x - 7529$	3.9	0.1140

[a]The coefficient of non-determination is the percent of variation which is unexplained by the regression equation

Figure caption

Figure 1. Dissolution profiles of diclofenac potassium film formulation.

Figure 2. Permeation profiles of diclofenac potassium film formulation across cornea at 34 °C

Figure 3. Influence of film on EPN, EPL, EPS and TAP of corneal permeation.

Figure 4. Means chart of observed versus predicted EPN, EPL, EPS and TAP of four formulations.

Figure 5. Correlation of *in vitro* dissolution and steady state *ex vivo* permeation at the same time point

Figure 6. Scanning electron micrographs of diclofenac potassium pure drug crystals (DCP) 5000×; and film formulations in HPMC matrix: (L1) 5000×; (L2) 5000×; (L3) 5000×; (L4) 5000×.

Figure. 7. (a) XRD pattern and (b) DSC thermograms of pure drug (DCP) and film formulations.

Figure 8. Conjunctival anti-inflammatory study: (a) carrageenan injection to upper palpebral region of eye; (b) normal rabbit eye before injection; (c) inflammatory condition of the eye after 1 hour of injection (acute inflammation); (d) just after applying hydrogel film in the eye; (e) after 1 hour of film application (inflammation subsided partially and the film has been partially swelled and eroded); (f) 2 hour after film application (inflammation subsided almost fully and residual film is left); (g) film dimension used for the study.

Figure 9.(a) Pdb structure of DCP; (b) Pdb structure of HPMC; (c) Docked structure of DCP and HPMC.

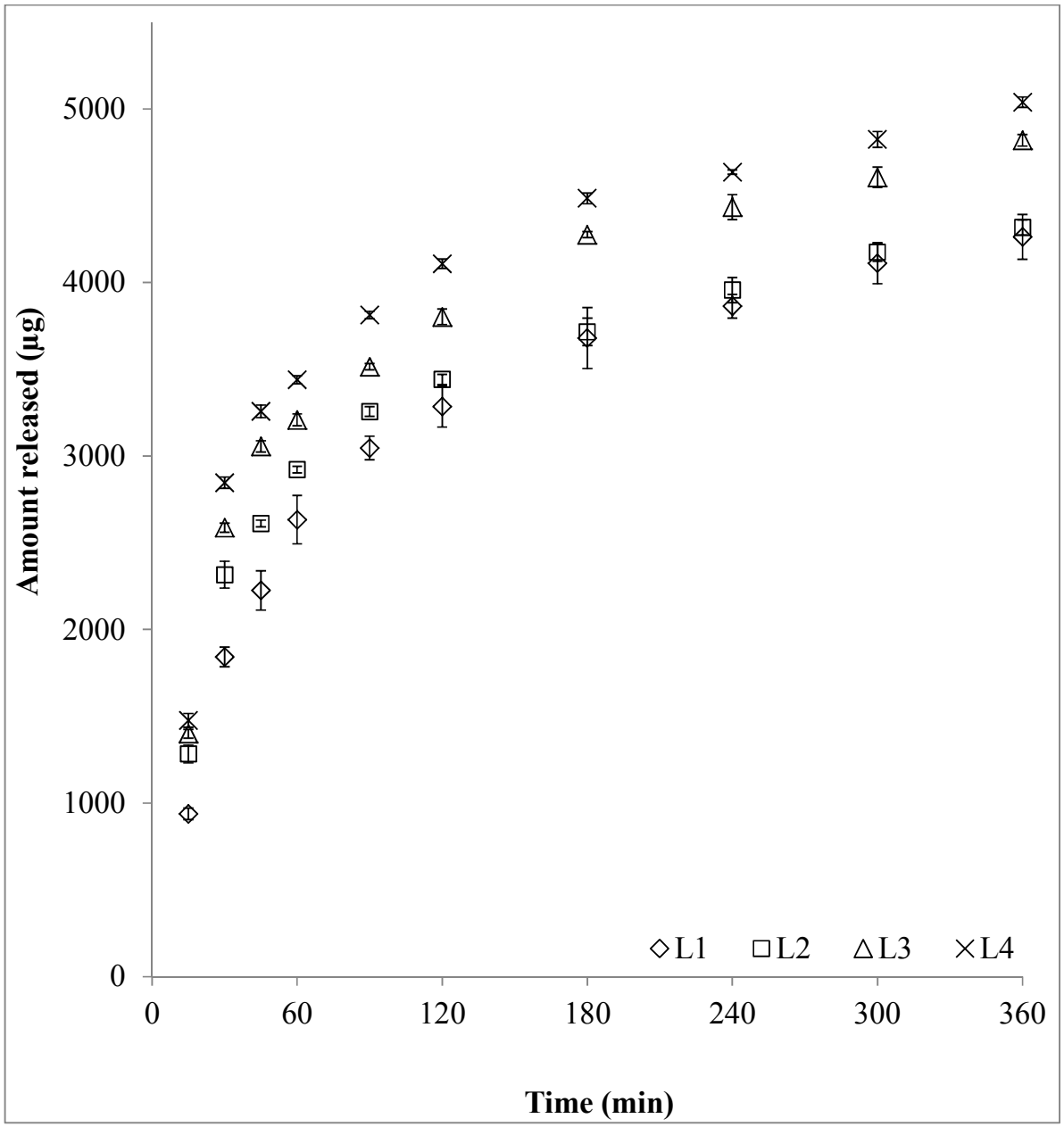

Figure 1. Dissolution profiles of diclofenac potassium film formulation

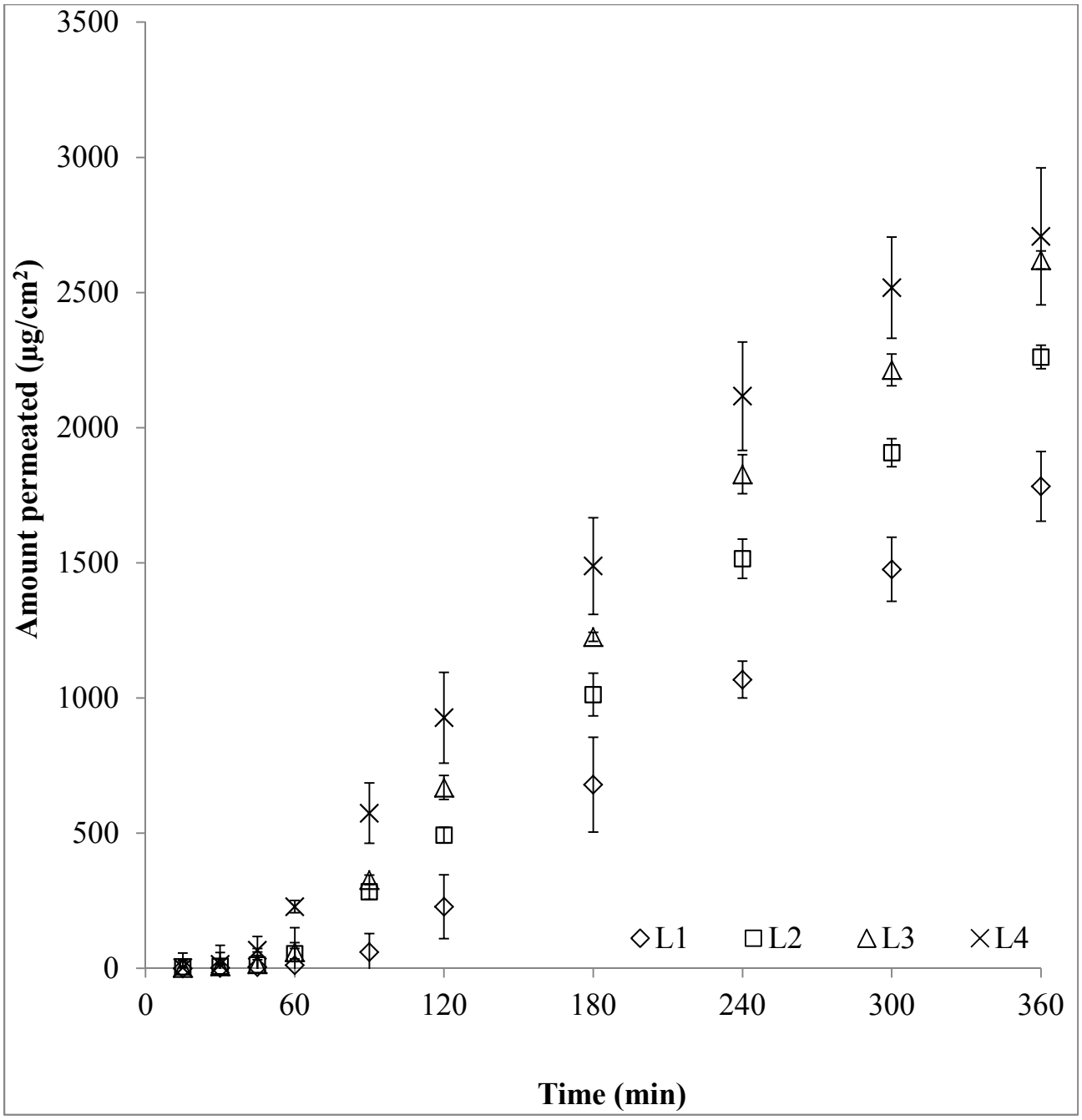

Figure 2. Permeation profiles of diclofenac potassium film formulation across cornea at 34 °C

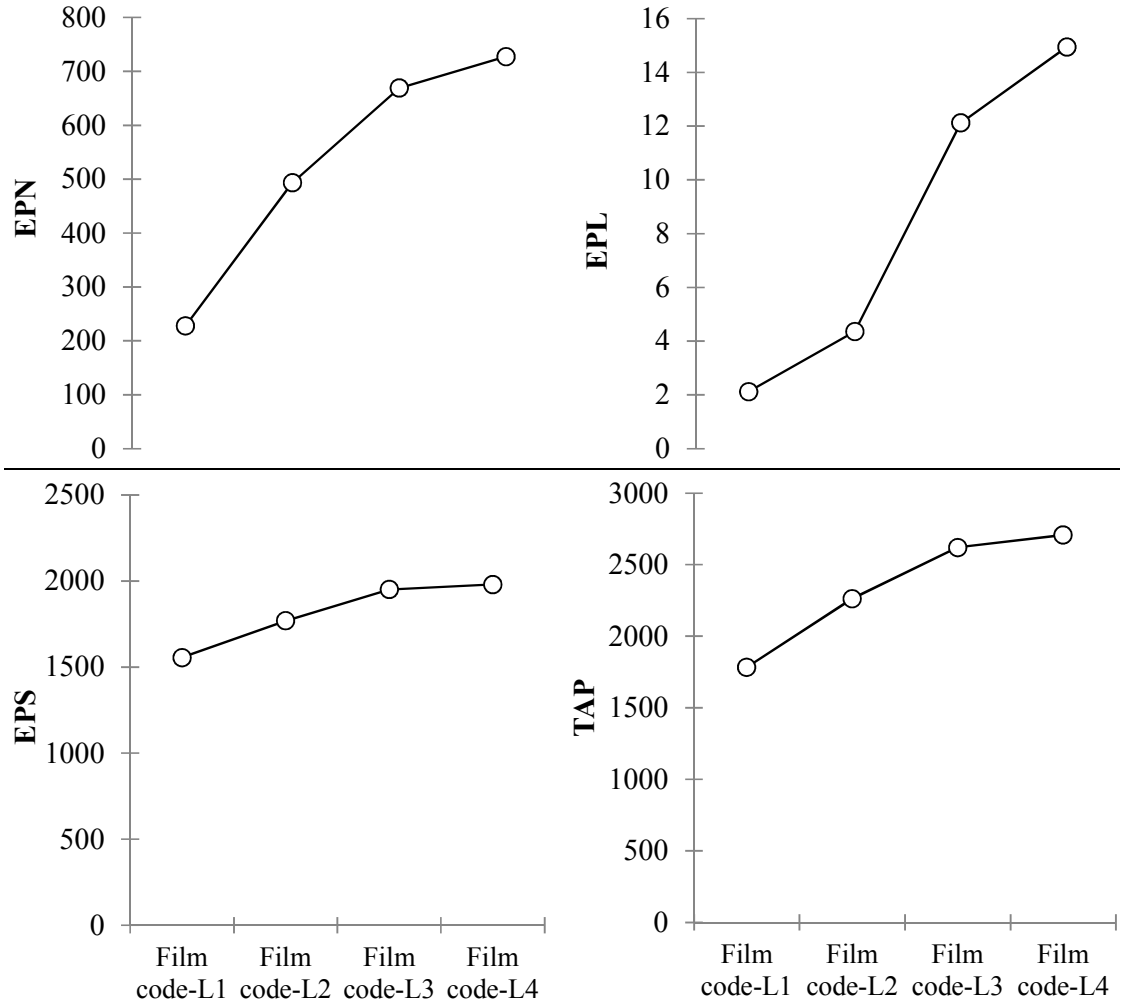

Figure 3. Influence of film on EPN, EPL, EPS and TAP of corneal permeation.

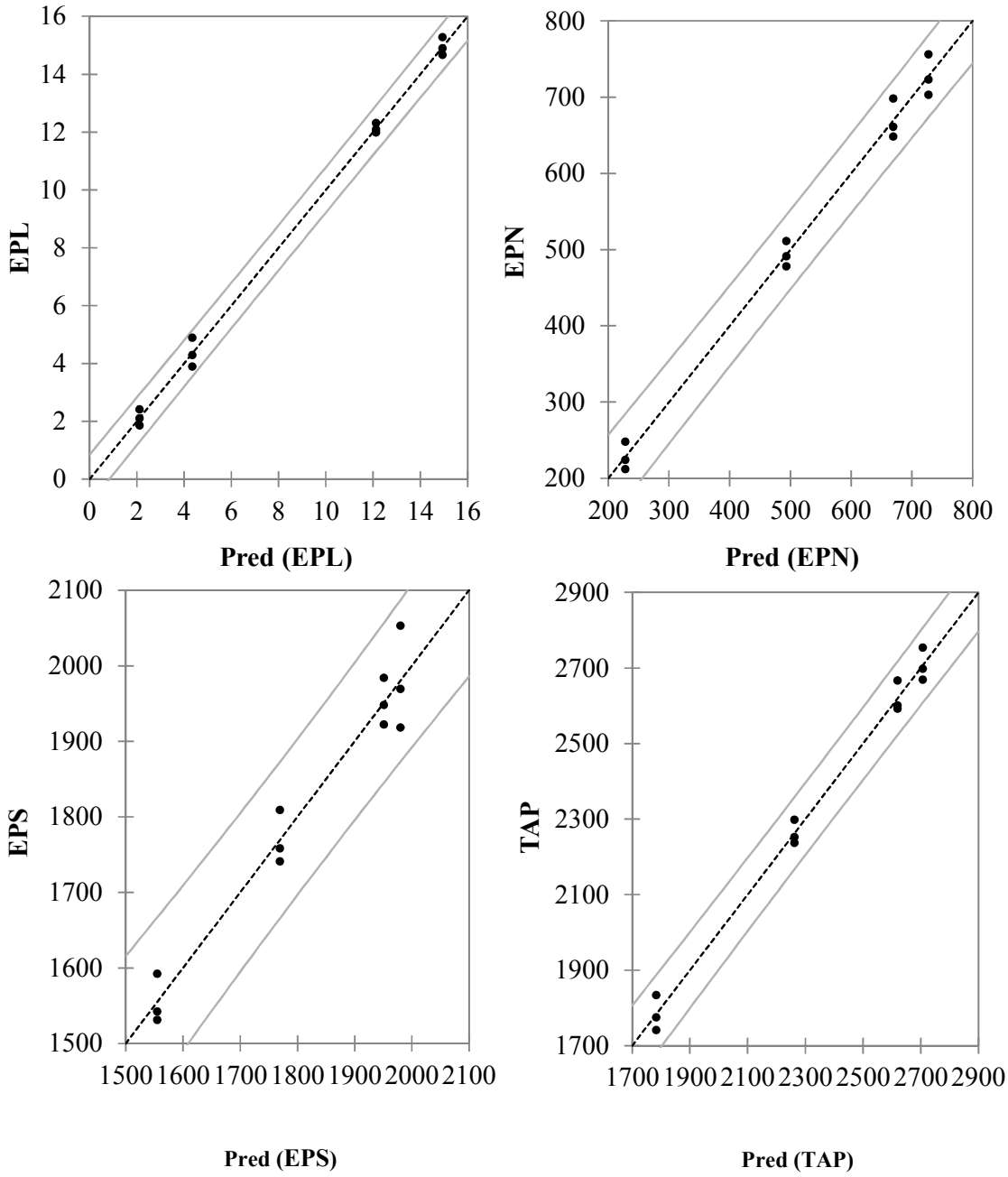

Figure 4. Means chart of observed versus predicted EPN, EPL, EPS and TAP of four formulations.

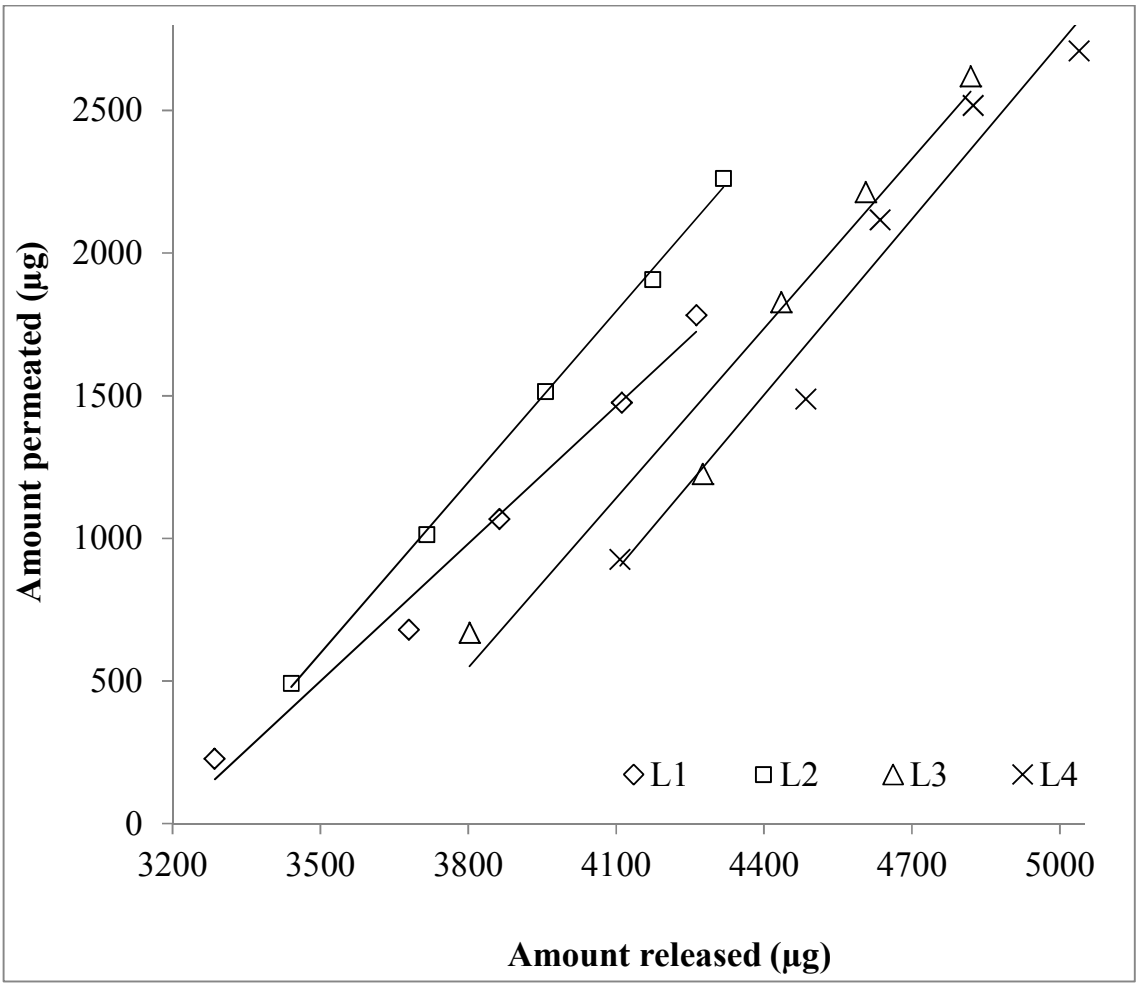

Figure 5. Correlation of *in vitro* dissolution and steady state *ex vivo* permeation at the same time point.

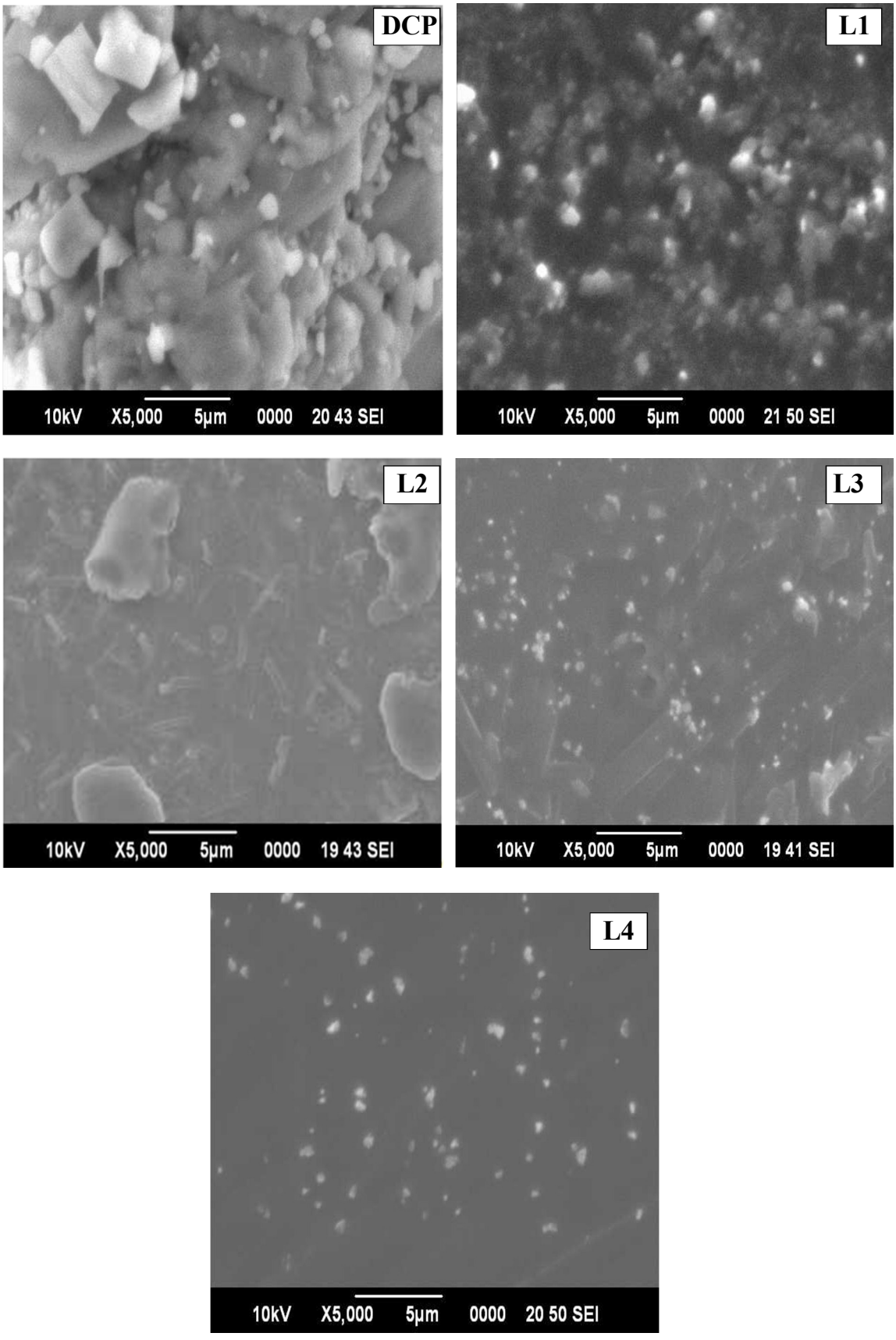

Figure 6. Scanning electron micrographs of diclofenac potassium pure drug crystals (DCP) 5000×; and film formulations in HPMC matrix: (L1) 5000×; (L2) 5000×; (L3) 5000×; (L4) 5000×.

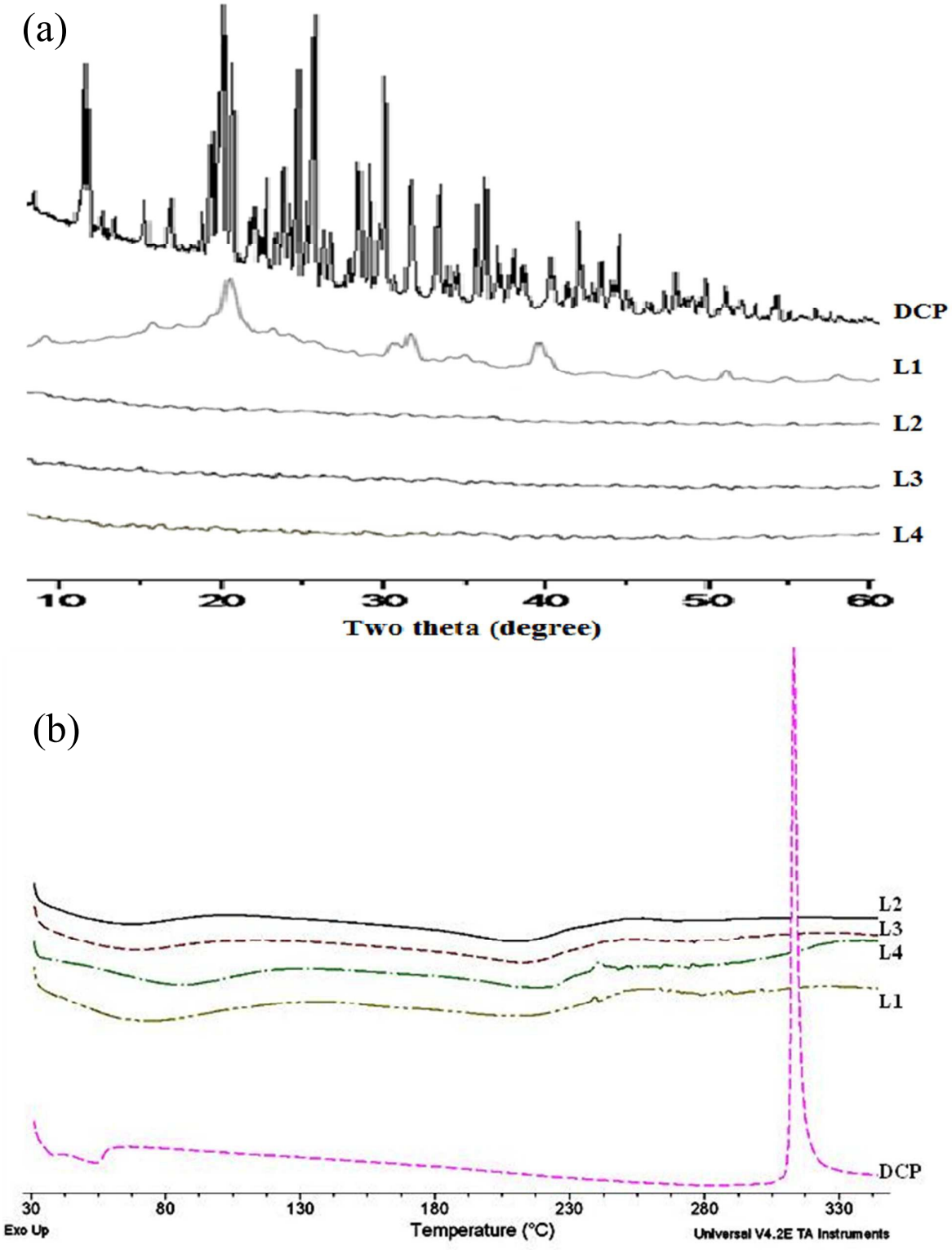

Figure. 7. (a) XRD pattern and (b) DSC thermograms of pure drug (DCP) and film formulations.

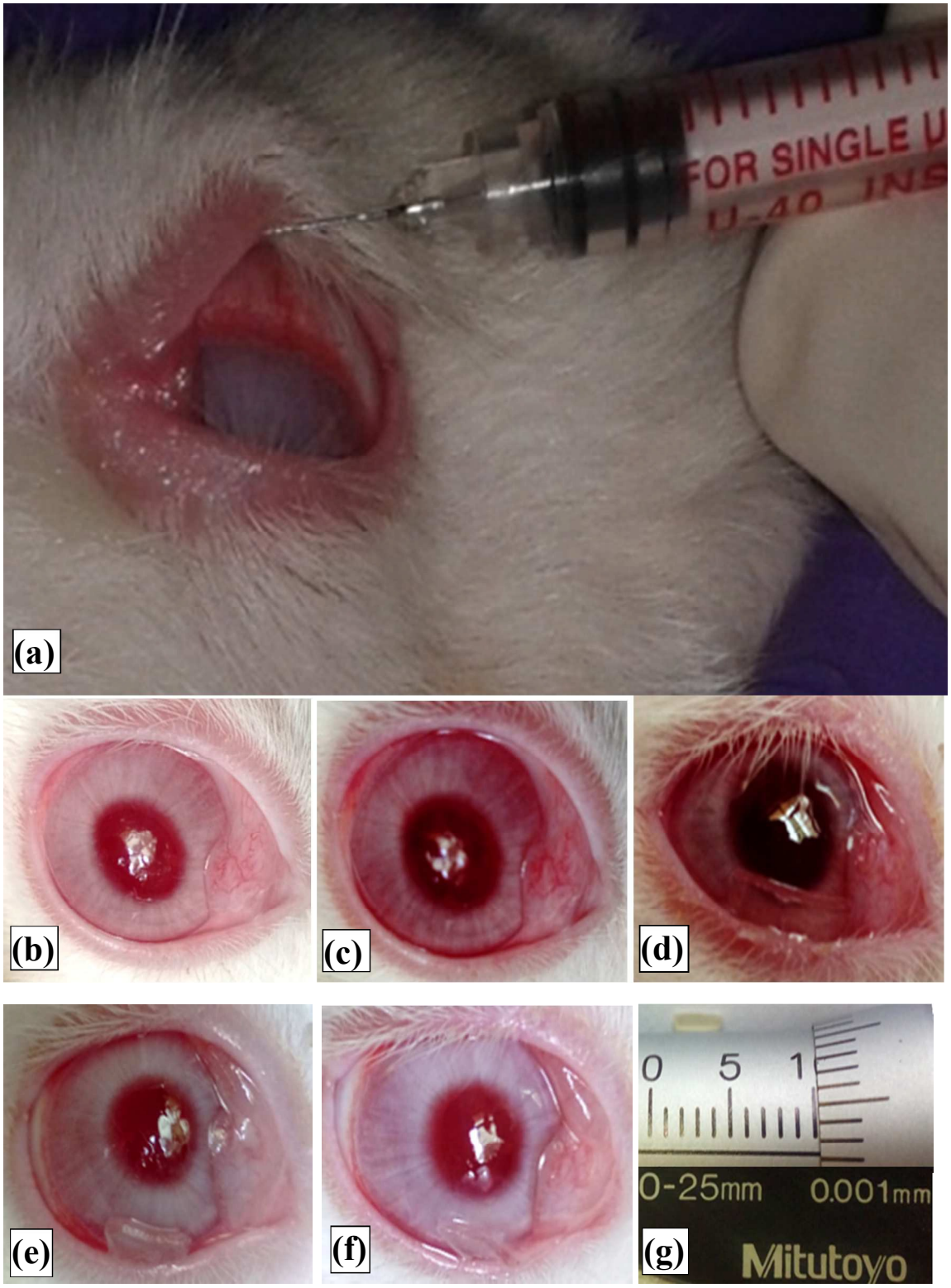

Figure 8. Conjunctival anti-inflammatory study: (a) carrageenan injection to upper palpebral region of eye; (b) normal rabbit eye before injection; (c) inflammatory condition of the eye after 1 hour of injection (acute inflammation); (d) just after applying hydrogel film in the eye; (e) after 1 hour of film application (inflammation subsided partially and the film has been partially swelled and eroded); (f) 2 hour after film application (inflammation subsided almost fully and residual film is left); (g) film dimension used for the study.

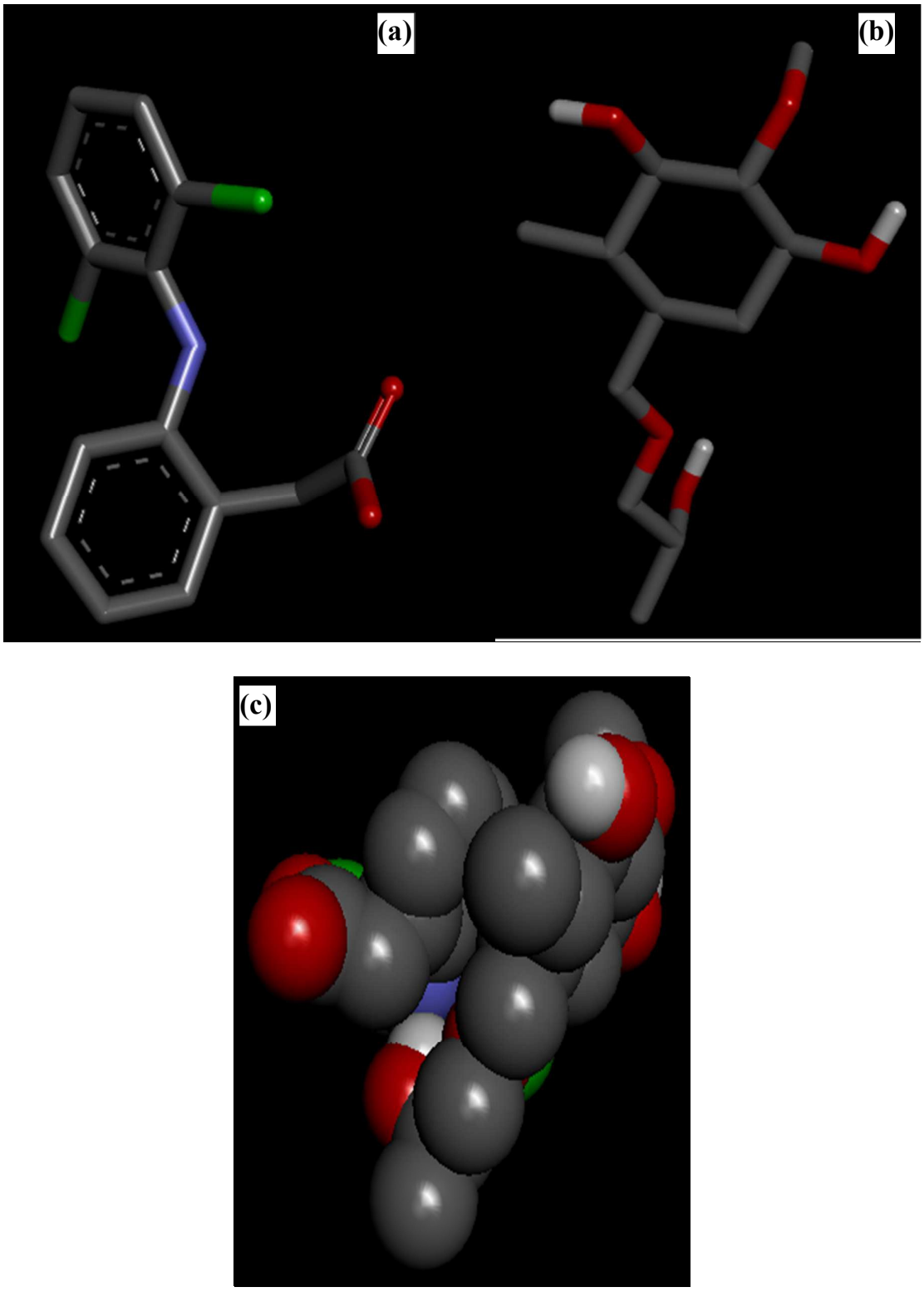

Figure 9. (a) Pdb structure of DCP; (b) Pdb structure of HPMC; (c) Docked structure of DCP and HPMC.

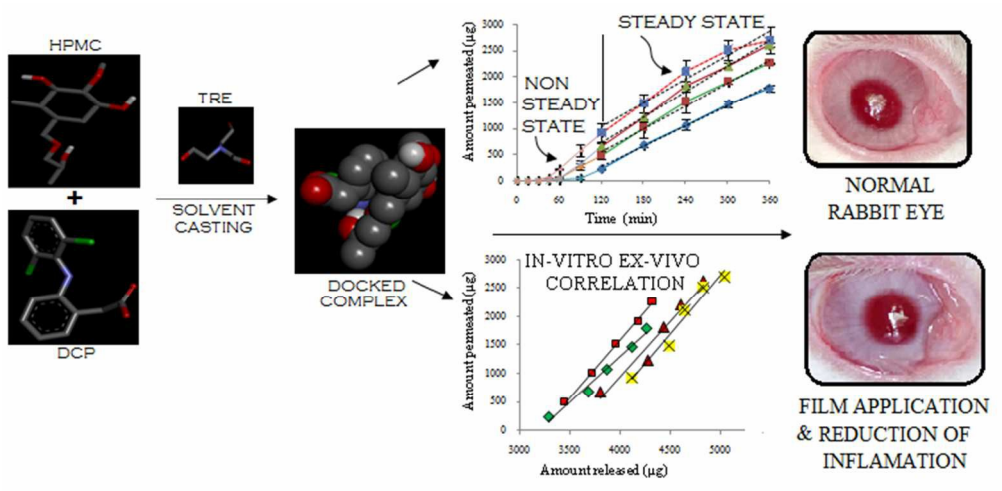

200x97mm (96 x 96 DPI)